

ρ -meson properties in medium

J. P. B. C. de Melo ^a, K. Tsushima ^a

^a*Laboratório de Física Teórica e Computacional - LFTC, Universidade Cruzeiro do Sul, 01506-000 São Paulo, Brazil*

Abstract

Properties of ρ -meson in symmetric nuclear matter are investigated in a light-front constituent quark model (LFCQM), using the in-medium inputs calculated by the quark-meson coupling (QMC) model. The LFCQM used in this study was already applied for the studies of the electromagnetic properties of ρ -meson in vacuum, namely, the charge G_0 , magnetic G_1 , and quadrupole G_2 form factors, electromagnetic charge radius, and electromagnetic decay constant. We predict that the electromagnetic decay constant, charge radius, and quadrupole moment are enhanced as increasing the nuclear matter density, while the magnetic moment is slightly quenched. Furthermore, we predict that the value Q_{zero}^2 , which crosses zero of the charge form factor, $G_0(Q_{\text{zero}}^2) = 0$ ($Q^2 = -q^2 > 0$ with q being the four-momentum transfer), decreases as increasing the nuclear matter density.

Key words: ρ -meson in medium, Electromagnetic form factors, Symmetric nuclear matter, Light-front constituent quark model, Quark-meson coupling model

1 Introduction

One of the fundamental objectives in hadronic physics is to understand the structure of hadrons in terms of the quark and gluon degrees of freedom, the basis of quantum chromodynamics (QCD). The Standard Model (SM) of elementary particles contains QCD as the strong interaction theory, and practicing QCD to understand the hadron structure is an important part of understanding SM. However, it is not straightforward to apply QCD directly to study the properties of hadrons such as mesons, baryons, and tetra-quarks, the bound state systems of quarks and gluons, in particular in the low energy nonperturbative region (see Ref. [1,2]). Despite many successes of QCD which is believed as the correct quantum field theory of strong interaction [3,4],

the hadronic properties in the low-energy region cannot be directly extracted naively. To overcome the difficulties, effective treatments of QCD, such as constituent quark models (CQM), light-front treatment of hadrons, have been developed and achieved impressive success [5-27]. In particular, we emphasize the cases of spin-1 vector particles [28-45], that are relevant for the present study of ρ -meson.

For the ρ -meson, experimental data are very scarce at present. In Ref. [46,47] some properties of the ρ -meson in medium were discussed based on the experiment data. Recently, in Ref. [48,49] the data from BaBar Collaboration [50] for the $e^+e^- \rightarrow \rho^+\rho^-$ reaction in vacuum were analyzed in order to study the electromagnetic properties of the ρ -meson based on perturbative QCD.

Light-front quantum field theory (LFQFT) on which the present study bases, is able to incorporate the following two important aspects simultaneously, namely, QCD and the picture of constituent quark model. It is a natural approach to calculate physical observables based on the quark degrees of freedom [3,4]. In the light-front approach one can have relativistic wave functions of the hadronic bound states described in terms of quarks and gluons, and the approach is suitable for understanding the hadron substructure focusing on nonperturbative aspect [28,49,51,52,53,54,55].

Based on the advantages mentioned above for the light-front approach, we use a light-front constituent quark model (LFCQM) which was already applied for the studies of ρ -meson electromagnetic properties in vacuum [35,56,57]. We extend the preliminary study made in symmetric nuclear matter for the ρ -meson properties in medium, and elaborate in the present work [58]. Namely, we calculate the ρ -meson electromagnetic charge G_0 , magnetic G_1 , and quadrupole G_2 form factors, electromagnetic square charge radius r_ρ^2 , and $\rho^0 \rightarrow e^+e^-$ decay constant f_ρ in symmetric nuclear matter. For this we use the plus-component of the electromagnetic current J_ρ^+ , under the situation that the ρ -meson is immersed in symmetric nuclear matter [59,60,61]. (For comprehensive reviews on hadronic and quark properties in nuclear medium, we refer the readers to e.g., Refs. [59,60].) The model for the ρ -meson in vacuum we use here [35], is constrained by the “angular condition” for the light-front electromagnetic current matrix elements [28,29,35,56,57,62]. Any light-front-based models of spin-1 particles should satisfy the angular condition, which was originally discussed in Ref. [63].

2 Quark-meson coupling model

To describe symmetric nuclear matter (many nucleon system), we rely on the quark-meson coupling (QMC) model, which bases on the quark degrees of free-

dom, and calculate necessary in-medium inputs for the quarks and hadrons to implement in the light-front constituent quark model, similarly to the studies made for pion and kaon [61,64,65,66] and nucleon [24]. Detail of the light-front constituent quark model we use in this study is described in Refs. [8,9,23] (and for nucleon in Ref. [24]).

The QMC model was invented by Guichon [67] using the MIT bag model, and Frederico et al. [68] using a relativistic confining harmonic potential. The model was successfully applied for studying the properties of finite nuclei [69], and the properties of hadrons in medium [70,71]. (See Ref. [70] for other approaches similar to the QMC model used in this study.) In the QMC model the meson and baryon internal structure is modified in medium due to the surrounding medium, by the self-consistent exchange of the scalar-isoscalar (σ), vector-isoscalar (ω), and vector-isovector (ρ) meson fields directly coupled to the relativistic, confined light-quarks in the nucleon (hadron), rather than to the point-like nucleon (hadron). We briefly explain next the main feature of the QMC model, which is used to calculate the in-medium inputs necessary to study the ρ -meson properties in symmetric nuclear matter.

We consider a system of infinite, uniform, spin and isospin saturated symmetric nuclear matter in the Hartree mean field approximation in the rest frame of matter. Thus, irrelevant ρ -meson field is suppressed in the following, since the total isospin of the matter is zero, and in the Hartree approximation ρ -meson mean field becomes zero. In addition quantities with an asterisk, *, will stand for those in medium hereafter. The effective Lagrangian density in the QMC model at the hadron level may be given by [70],

$$\mathcal{L} = \bar{\psi}[i\gamma \cdot \partial - m_N^*(\hat{\sigma}) - g_\omega \hat{\omega}^\mu \gamma_\mu]\psi + \mathcal{L}_{\text{meson}}, \quad (1)$$

with $\mathcal{L}_{\text{meson}}$ being the free meson Lagrangian,

$$\mathcal{L}_{\text{meson}} = \frac{1}{2}(\partial_\mu \hat{\sigma} \partial^\mu \hat{\sigma} - m_\sigma^2 \hat{\sigma}^2) - \frac{1}{2}\partial_\mu \hat{\omega}_\nu (\partial^\mu \hat{\omega}^\nu - \partial^\nu \hat{\omega}^\mu) + \frac{1}{2}m_\omega^2 \hat{\omega}^\mu \hat{\omega}_\mu.$$

In the above ψ , $\hat{\sigma}$ and $\hat{\omega}$ are respectively the nucleon, Lorentz-scalar-isoscalar σ , and Lorentz-vector-isoscalar ω field operators, with g_ω being the nucleon- ω coupling constant, while the nucleon- σ effective coupling which depends on the $\hat{\sigma}$ (or nuclear density) is defined by,

$$m_N^*(\hat{\sigma}) = m_N - g_\sigma(\hat{\sigma})\hat{\sigma}, \quad (2)$$

where the effective nucleon mass is denoted by m_N^* . Then, the nucleon density ρ_N and the nucleon Fermi momentum k_F , the nucleon scalar density ρ_s , and the effective nucleon mass m_N^* are related by,

$$\begin{aligned}\rho_N &= \frac{4}{(2\pi)^3} \int d\vec{k} \theta(k_F - |\vec{k}|) = \frac{2k_F^3}{3\pi^2}, \\ \rho_s &= \frac{4}{(2\pi)^3} \int d\vec{k} \theta(k_F - |\vec{k}|) \frac{m_N^*(\sigma)}{\sqrt{m_N^{*2}(\sigma) + \vec{k}^2}},\end{aligned}\quad (3)$$

where $m_N^*(\sigma)$ is the value of the effective nucleon mass at a given density, calculated by the QMC model [69,70].

The Dirac equations for the light quarks and light antiquarks in the bag of hadron h in nuclear matter at the position $x = (t, \vec{r})$ with $|\vec{r}| \leq \text{bag radius}$, are given by [70],

$$\begin{aligned}\left[i\gamma \cdot \partial_x - (m_q - V_\sigma^q) \mp \gamma^0 \left(V_\omega^q + \frac{1}{2} V_\rho^q \right) \right] \begin{pmatrix} \psi_u(x) \\ \psi_{\bar{u}}(x) \end{pmatrix} &= 0, \\ \left[i\gamma \cdot \partial_x - (m_q - V_\sigma^q) \mp \gamma^0 \left(V_\omega^q - \frac{1}{2} V_\rho^q \right) \right] \begin{pmatrix} \psi_d(x) \\ \psi_{\bar{d}}(x) \end{pmatrix} &= 0,\end{aligned}\quad (4)$$

where, $V_\sigma^q = g_\sigma^q \sigma$, $V_\omega^q = g_\omega^q \omega$, and $V_\rho^q = g_\rho^q b$ are respectively the constant mean field potentials with the corresponding quark-meson coupling constants, g_σ, g_ω and g_ρ^q , and the Coulomb interactions are neglected, because the nuclear matter is described in the strong interaction. The vector meson mean fields appearing in V_ω^q and V_ρ^q , correspond respectively to the expectation values evaluated in symmetric nuclear matter, $\omega^\mu = (\omega, \vec{0})$ and $\rho_i^\mu = (\delta_{i,3} b, \vec{0})$. In addition SU(2) symmetry for the light-quark masses, $m_q = m_{\bar{q}} = m_u = m_d$, is assumed.

The normalized, static solution for the ground state light quark (q) and light antiquark (\bar{q}) in the hadron h may be written as $\psi_{q,\bar{q}}(x) = N_{q,\bar{q}} e^{-i\epsilon_{q,\bar{q}} t/R_h^*} \psi_{q,\bar{q}}(\vec{r})$, where $N_{q,\bar{q}}$ and $\psi_{q,\bar{q}}(\vec{r})$ are the normalization factor and corresponding spin and spatial part of the wave function. The bag radius in medium of the hadron h , R_h^* , is determined by the stability condition for the mass of the hadron against the variation of the bag radius [70], to be shown in Eq. (6). The eigenenergies in units of $1/R_h^*$ are given by,

$$\begin{aligned}\begin{pmatrix} \epsilon_u \\ \epsilon_{\bar{u}} \end{pmatrix} &= \Omega_q^* \pm R_h^* \left(V_\omega^q + \frac{1}{2} V_\rho^q \right), \\ \begin{pmatrix} \epsilon_d \\ \epsilon_{\bar{d}} \end{pmatrix} &= \Omega_q^* \pm R_h^* \left(V_\omega^q - \frac{1}{2} V_\rho^q \right),\end{aligned}\quad (5)$$

where, $\Omega_q^* = \Omega_{\bar{q}}^* = [x_q^2 + (R_h^* m_q^*)^2]^{1/2}$, with $m_q^* = m_q - g_\sigma^q \sigma$, and x_q being the lowest bag eigenfrequency. Because we consider symmetric nuclear matter with the Hartree approximation, V_ρ^q is zero also at the quark level, thus we will ignore hereafter.

The mass of the low-lying hadron h in symmetric nuclear matter, is calculated with the bag radius stability condition,

$$m_h^* = \sum_{j=q,\bar{q}} \frac{n_j \Omega_j^* - z_h}{R_h^*} + \frac{4}{3} \pi R_h^{*3} B, \quad \left. \frac{\partial m_h^*}{\partial R_h} \right|_{R_h=R_h^*} = 0, \quad (6)$$

with $n_q(n_{\bar{q}})$ being the light-quark (light-antiquark) number.

Now we study the ρ -meson properties in symmetric nuclear matter using the inputs calculated by the QMC model. To do so, we must rely on the ρ -meson model in vacuum which is successful and simple enough to handle for extracting the main in-medium properties. As already mentioned, we use the light-front constituent quark model for the ρ -meson developed in Ref. [35].

The model uses the light-quark constituent quark mass value in vacuum $m_q = m_{\bar{q}} = 430$ MeV. Using this value we calculate the corresponding symmetric nuclear matter properties with the QMC model. By fitting the nuclear matter saturation properties, namely the binding energy of 15.7 MeV at the saturation density $\rho_0 = 0.15 \text{ fm}^{-3}$, we obtain the corresponding quark-meson coupling constants. The coupling constants, and some quantities calculated in the QMC model at ρ_0 are listed in Tab. 1. For a comparison, the same quantities obtained in the standard QMC model with $m_q = 5$ MeV, are also listed in Tab. 1.

Table 1

The QMC model (MIT bag model) quantities (see Ref. [70] for details), coupling constants, the parameters z_N (z_ρ) for nucleon (ρ -meson) [see Eq. (6)], bag constant B ($B^{1/4}$ in [MeV]), and some properties for symmetric nuclear matter at normal nuclear matter density $\rho_0 = 0.15 \text{ fm}^{-3}$, for $m_q = 5$ and 430 MeV (the latter is relevant for this study). The effective nucleon (quark) mass, m_N^* (m_q^*), and the nuclear incompressibility, K , are quoted in [MeV]. The free nucleon bag radius is the input with $R_N = 0.8$ fm, the standard value in the QMC model [70]. The vacuum mass value (input) for the ρ -meson is $m_\rho = 770$ MeV.

m_q (MeV)	$g_\sigma^2/4\pi$	$g_\omega^2/4\pi$	m_N^*	m_q^*	K	z_N	z_ρ	$B^{1/4}$
5	5.39	5.30	754.6	-135.6	279.3	3.295	1.907	170.0
430	8.73	11.94	565.3	245.7	361.4	5.497	2.939	69.8

One of the noticeable differences among the quantities calculated with the standard value $m_q = 5$ MeV and those with the value $m_q = 430$ MeV, is the nuclear incompressibility, K . It yields a larger value of $K = 361.4$ MeV with $m_q = 430$ MeV, while $K = 279.3$ MeV with $m_q = 5$ MeV. The corresponding energy density per nucleon for $m_q = 430$ MeV, $(E^{\text{Total}}/A) - m_N$, is shown in Fig. 1 upper panel.

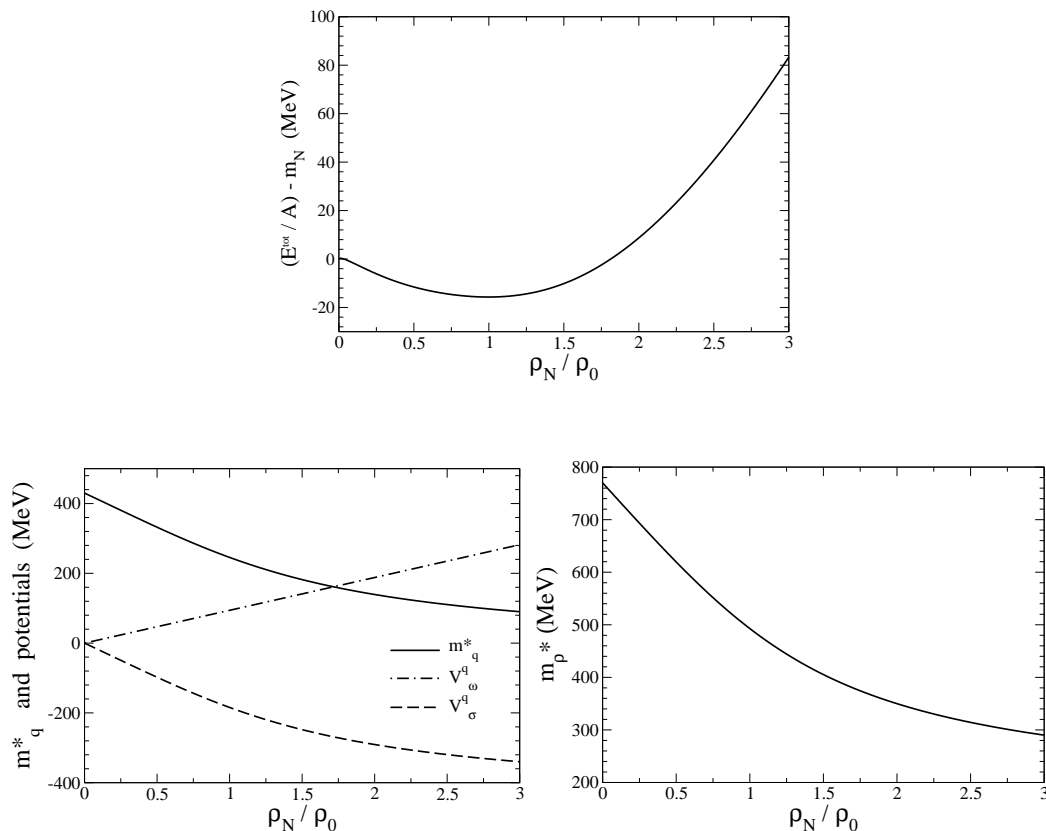


Fig. 1. Energy per nucleon $(E^{\text{Total}}/A) - m_N$ (upper panel), effective quark masses and the potentials felt by the light quarks (lower-left panel), and effective ρ -meson mass (lower-right panel) in symmetric nuclear matter calculated in the QMC model [70].

Concerning the solid line shown in Fig. 1 upper panel, the curvature of the energy density versus ρ/ρ_0 is larger than that for $m_q = 5$ MeV. Thus $(E^{\text{Total}}/A) - m_N$ varies faster than that for $m_q = 5$ MeV as the nuclear matter density increases. (See Ref. [70] for the curve of $(E^{\text{Total}}/A) - m_N$ with $m_q = 5$ MeV.) Next, we show also in Fig. 1 lower-left panel the effective light-quark mass $m_q^* = m_q - g_\sigma^q \sigma$, scalar potential $V_\sigma^q = g_\sigma^q \sigma$, and vector potential $V_\omega^q = g_\omega^q \omega$ felt by the light quarks, and in lower-right panel the effective ρ -meson mass m_ρ^* . (See Eq. (6) for m_ρ^* with $h \rightarrow \rho$.) Note that, the ρ -meson effective mass m_ρ^* shown in Fig. 1 lower-right panel, corresponds to that of naive SU(6) quark models, and readers must not be confused with that of the ρ -meson mean field (operator) appearing in the QMC model. In addition we have neglected the width of the ρ -meson, following the usual treatment of naive SU(6) quark

models.

3 ρ -meson electromagnetic form factors

A general expression of the electromagnetic current for a ρ -meson (spin-1 particle) is given by [72]:

$$J_{\alpha\beta}^\mu = - \left[F_1(Q^2)g_{\alpha\beta} - F_3(Q^2)\frac{q_\alpha q_\beta}{2m_\rho^2} \right] P^\mu - F_M(Q^2) (q_\alpha g_\beta^\mu - q_\beta g_\alpha^\mu), \quad (7)$$

where m_ρ is the mass of the ρ -meson, q^μ the four-momentum transfer with $Q^2 = -q^2 > 0$, and $P^\mu \equiv (p_i + p_f)^\mu$, the sum of the initial (p_i) and final (p_f) momenta. The electromagnetic current, $J_{ji}^\mu \equiv \epsilon_j'^\alpha J_{\alpha\beta}^+ \epsilon_i^\beta$, in an impulse approximation is given by,

$$J_{ji}^\mu = i \int \frac{d^4 k}{(2\pi)^4} \frac{\text{Tr}[\epsilon_j'^\alpha \Gamma_\alpha(k, k - p_f)(\not{k} - \not{p}_f + m_q)\gamma^\mu(\not{k} - \not{p}_i + m_q)]}{((k - p_i)^2 - m_q^2 + i\epsilon)(k^2 - m_q^2 + i\epsilon)((k - p_f)^2 - m_q^2 + i\epsilon)} \epsilon_i^\beta (\not{k} + m_q) \Gamma_\beta(k, k - p_i) \times \Lambda(k, p_f) \Lambda(k, p_i), \quad (8)$$

where m_q is the quark mass, and without loss of generality, the four-momenta of the initial and final states of the ρ -meson may respectively be chosen by $p_i^\mu = (p^0, -q/2, 0, 0)$ and $p_f^\mu = (p^0, q/2, 0, 0)$ with the four-momentum transfer defined by $q^\mu = (0, q, 0, 0)$ to satisfy the Drell-Yan condition [29,35]. In Eq. (8) $\epsilon_j'^\alpha$ and ϵ_i^β are the final- and initial-state ρ -meson polarization vectors, respectively given by,

$$\epsilon_x'^\mu = (\sqrt{\eta}, \sqrt{1 + \eta}, 0, 0), \quad \epsilon_y'^\mu = (0, 0, 1, 0), \quad \epsilon_z'^\mu = (0, 0, 0, 1), \quad (9)$$

and

$$\epsilon_x^\mu = (-\sqrt{\eta}, \sqrt{1 + \eta}, 0, 0), \quad \epsilon_y^\mu = (0, 0, 1, 0), \quad \epsilon_z^\mu = (0, 0, 0, 1), \quad (10)$$

with $\eta = Q^2/m_\rho^2$. The electromagnetic current, Eq. (8), is divergent, and in order to make J_{ji}^μ finite, a regulator function $\Lambda(k, p)$ is used [35]:

$$\Lambda(k, p) = \frac{1}{((k - p)^2 - m_R^2 + i\epsilon)^2}. \quad (11)$$

Here, the regulator mass value m_R is chosen to reproduce the experimental value of the ρ -meson decay constant f_ρ (see Eq. (19) for the definition) extracted from the $\rho^0 \rightarrow e^+ e^-$ decay width [73]. The ρ - $q\bar{q}$ vertex with spinor structure is modeled by [35],

$$\Gamma^\mu(k, k') = \gamma^\mu - \frac{m_\rho}{2} \frac{k^\mu + k'^\mu}{p \cdot k + m_\rho m_q - i\epsilon}, \quad (12)$$

where the ρ -meson is on-mass-shell, and its four momentum is $p^\mu = k^\mu - k'^\mu$ with the quark momenta k^μ and k'^μ [29,35].

Working with the light-front coordinate, $a^\mu = (a^+ = a^0 + a^3, a^- = a^0 - a^3, \vec{a}_\perp = (a^1, a^2))$, the light-front ρ -meson wave function is obtained, after substituting with the on-mass-shell condition $k^- = (k_\perp^2 + m_q^2)/k^+$ in the quark propagator (see Ref. [35] for details),

$$\Phi_i(x, \vec{k}_\perp) = \frac{N^2}{(1-x)^2(m_\rho^2 - M_0^2)(m_\rho^2 - M_R^2)^2} \vec{\epsilon}_i \cdot [\vec{\gamma} - \frac{\vec{k}}{\frac{M_0}{2} + m_q}] , \quad (13)$$

where, $x = k^+/p^+$. The polarization state is given by $\vec{\epsilon}_i$. The wave function corresponds to an S-wave state [51]. The square of the free mass operator M_0^2 , and the regulator mass operator M_R^2 , are given by:

$$M_0^2 = \frac{k_\perp^2 + m_q^2}{x} + \frac{(\vec{p} - \vec{k})_\perp^2 + m_q^2}{1-x} - \vec{p}_\perp^2, \quad (14)$$

$$M_R^2 = \frac{k_\perp^2 + m_q^2}{x} + \frac{(\vec{p} - \vec{k})_\perp^2 + m_R^2}{1-x} - \vec{p}_\perp^2. \quad (15)$$

3.1 Angular condition and electromagnetic form factors

For the spin-1 particles in the light-front approach, matrix elements of the plus-component of electromagnetic current, J^+ , is constrained by the angular condition equation with the light-front spin basis [28,35,63]:

$$\Delta(q^2 = -Q^2) = (1 + 2\eta)I_{11}^+ + I_{1-1}^+ - \sqrt{8\eta}I_{10}^+ - I_{00}^+ = 0. \quad (16)$$

The relations among the light-front basis $I_{m'm}^+$ ($m', m = \pm 1, 0$) and those of the instant form spin basis J_{ji}^+ ($j, i = x, y, z$), can be made by the Melosh rotation matrix. (See Ref. [29,35] for details.)

With the angular condition Eq. (16), it is possible to arrange the electromagnetic form factors to form with different linear combinations [28,35] by eliminating some matrix elements $I_{m'm}^+$. However, some linear combinations break the covariance as well as the rotational symmetry. This is due to the zero mode contributions, or pair term contributions [29,74,75]. In Ref. [29] a careful analysis was made for the origins of the zero-mode contributions for the matrix elements of the electromagnetic current of spin-1 particles, in particular for the ρ -meson.

It was demonstrated that the zero mode contributions are canceled out in the combinations of the electromagnetic current matrix elements of Grach et al. [63], by numerically in Ref. [35], and by analytically in Ref. [29]. The reason is that the electromagnetic matrix element of the current, I_{00}^+ , was eliminated by the angular condition [28,35,36,63]. For some prescriptions in the literature, the zero-mode or non-valence contributions needed to be added in order to recover the full covariance [18,29,35,74].

With the prescription of Ref. [63], the electromagnetic form factors of ρ -meson are given by both in the light-front spin basis $I_{mm'}^+$ and the instant form spin basis J_{ji}^+ :

$$\begin{aligned} G_0 &= \frac{1}{3} \left[(3 - 2\eta) I_{11}^+ + 2\sqrt{2\eta} I_{11}^+ + I_{1-1}^+ \right] = \frac{1}{3} \left[J_{xx}^+ + 2J_{yy}^+ - \eta J_{yy}^+ + \eta J_{zz}^+ \right], \\ G_1 &= 2 \left[I_{11}^+ - \frac{1}{\sqrt{2\eta}} I_{10}^+ \right] = \left[J_{yy}^+ - J_{zz}^+ - \frac{J_{zx}^+}{\sqrt{\eta}} \right], \\ G_2 &= \frac{2\sqrt{2}}{3} \left[-\eta I_{11}^+ + \sqrt{2\eta} I_{10}^0 - I_{1-1}^+ \right] = \frac{\sqrt{2}}{3} \left[J_{xx}^+ - (1 + \eta) J_{yy}^+ + \eta J_{zz}^+ \right]. \end{aligned} \quad (17)$$

The electromagnetic form factors G_0 , G_1 and G_2 above, are related by the covariant form factors F_1 , F_M and F_3 of Eq. (7) [72]:

$$\begin{aligned} G_0 &= F_1(Q^2) + \frac{2}{3}\eta G_2(Q^2), \quad (\text{see below}), \\ G_1 &= F_M(Q^2), \\ G_2 &= F_1(Q^2) - F_M(Q^2) + (1 + \eta)F_3(Q^2). \end{aligned} \quad (18)$$

The ρ -meson decay constant, f_ρ , is defined by [18,52],

$$\langle 0 | \bar{q}(0) \gamma^\mu q(0) | \phi_\rho(\lambda) \rangle = \epsilon_\lambda^\mu m_\rho f_\rho, \quad (19)$$

where ϵ_λ^μ is the polarization vector of the corresponding ρ -meson state $\phi_\rho(\lambda)$. Note that f_ρ defined above has the mass dimension one, the same as the usual definition of the pion decay constant (but without a factor $\sqrt{2}$). Here, we use the plus-component of the electromagnetic current with $\lambda = z$ in the rest frame of the ρ -meson, and $e_z^+ = 1$ with $e_z^\mu = (e_z^+, e_z^-, \vec{e}_\perp) = (1, -1, \vec{0})$ [18]. The result is independent of the choice of λ .

We calculate also the ρ -meson magnetic moment μ_ρ , quadrupole moment $Q_{2\rho}$, and electromagnetic square charge radius $\langle r_\rho^2 \rangle$. They are obtained by the following expressions [72]:

$$1 = G_0(0), \text{ (charge normalization),} \quad (20)$$

$$\mu_\rho = G_1(0) = F_M(0), \quad (21)$$

$$Q_{2\rho} = G_2(0) \quad (22)$$

$$\langle r_\rho^2 \rangle = \lim_{Q^2 \rightarrow 0} \frac{-6 [G_0(Q^2) - 1]}{Q^2} = -6 \left. \frac{dG_0(Q^2)}{dQ^2} \right|_{Q^2=0} \quad (23)$$

4 Results

In the following we present the results for the in-medium ρ -meson properties calculated in symmetric nuclear matter, namely in-medium electromagnetic charge (G_0^*), magnetic (G_1^*), and quadrupole (G_2^*) form factors, electromagnetic square charge radius $\langle r_\rho^{*2} \rangle$, and electromagnetic ρ -meson decay constant f_ρ^* . These are calculated by the light-front constituent quark model, using the in-medium inputs obtained by the QMC model as already explained.

Before presenting the results, we briefly remind below how the ρ -meson properties are calculated in symmetric nuclear matter. As explained in section 2, the light-quark and light-antiquark self-energies in symmetric nuclear matter are modified by the Lorentz-scalar-isoscalar σ and Lorentz-vector-isoscalar ω mean fields. More specifically, in the Hartree approximation, the light-quark mass term acquires the attractive Lorentz scalar potential V_σ^q , while the time component of the light-quark (light-antiquark) four-momentum acquires the repulsive (attractive) mean field potential V_ω^q . Namely, the four-momentum p^μ of the light-quark (light-antiquark) is modified by, $p^\mu \rightarrow p^{*\mu} = p^\mu + V^\mu = p^\mu + \delta_0^\mu V_\omega^q$ ($p^\mu - \delta_0^\mu V_\omega^q$), and both the light-quark and light-antiquark masses are modified by $m_q \rightarrow m_q^* = m_q - V_\sigma^q = m_q - g_\sigma^q \sigma$. These mean field potentials are constrained by the nuclear matter saturation properties (see Fig. 1 upper panel). Then, using the in-medium modified light-quark (light-antiquark) properties, as well as the effective ρ -meson mass obtained in the QMC model (see Fig. 1 lower-right panel), we calculate the in-medium ρ -meson electromagnetic properties. Similar approach has already been applied for the studies of pion [61], kaon [66] and nucleon [24] properties in symmetric nuclear matter. In the loop integral appearing in the calculations of electromagnetic form factors or the decay constant, we shift the momentum, $k'^\mu = k^\mu + \delta_0^\mu V^0 \rightarrow k^\mu$, and the vector potentials cancel out for the light-quark and light-antiquark systems such as pion and ρ -meson.

Furthermore, since the effective ρ -meson mass decreases as increasing the nuclear matter density in the QMC model (see Fig. 1 right panel), the sum of the effective quark masses ($m_q^* + m_{\bar{q}}^*$) forming the ρ -meson bound state, must be larger than the in-medium ρ -meson mass (m_ρ^*), namely the binding energy (B^*) to be positive, the same condition as in vacuum, to be discussed in detail

later. We summarize in Tab. 2 some quantities calculated for the ρ -meson in symmetric nuclear matter.

Table 2

Quantities associated with the in-medium ρ -meson properties. Effective light-quark mass (m_q^*) and in-medium ρ -meson mass (m_ρ^*) are quoted in [GeV], while the ρ -meson electromagnetic square charge radius $\langle r_\rho^{*2} \rangle$ is in [fm²], the electromagnetic decay constant f_ρ^* in [MeV], the magnetic moment μ_ρ^* in units of [$e/2m_\rho$], quadrupole moment $Q_{2\rho}^*$ in [fm²], and the momentum Q_{zero}^2 for $G_0(Q_{\text{zero}}^2) = 0$ in [GeV²]. The experimental value for $\Gamma_{ee} \equiv \Gamma(\rho^0 \rightarrow e^+e^-) = 7.04 \pm 0.06$ keV in vacuum ($\rho_N = 0$) is taken from Ref. [73].

ρ/ρ_0	m_q^*	m_ρ^*	$\langle r_\rho^{*2} \rangle$	f_ρ^*	μ_ρ^*	$Q_{2\rho}^*$	Q_{zero}^2
0	0.430	0.770	0.267	153.627	2.20	-0.0590	2.96
0.01	0.427	0.767	0.270	153.669	2.20	-0.0595	2.96
0.10	0.410	0.738	0.296	163.206	2.20	-0.0639	2.74
0.25	0.381	0.692	0.352	166.148	2.19	-0.0721	2.43
0.40	0.351	0.640	0.433	174.499	2.19	-0.0817	2.14
0.50	0.333	0.618	0.505	179.325	2.18	-0.0884	1.97
0.75	0.285	0.552	0.895	176.796	2.15	-0.0994	1.57
0.80	0.278	0.538	1.214	178.739	2.14	-0.1028	1.53
0.85	0.268	0.527	1.353	189.556	2.12	-0.1134	1.48
0.90	0.260	0.514	1.857	195.042	2.10	-0.1152	1.40
Exp. [73]	for	Γ_{ee}	($\rho_N = 0$)	152±8			

To understand better the bound state nature in the present light-front constituent quark model, we discuss the binding energy, which should be positive in order to yield the bound state for the quark-antiquark composite system. The binding energy of the ρ -meson in medium B^* is defined by, $B^* = m_q^* + m_{\bar{q}}^* - m_\rho^*$. The binding energy calculated in symmetric nuclear matter is shown in Fig. 2, versus the nuclear matter density ρ_N/ρ_0 (upper panel), versus the effective light-quark mass m_q^* (lower-left panel), and versus the ρ -meson effective mass m_ρ^* (lower-right panel).

The dependence of the binding energy on the nuclear matter density, effective quark mass and effective ρ -meson mass, are all nearly linear and smooth. As the nuclear matter density increases, the binding energy B^* decreases, and the density beyond about $\rho/\rho_0 = 0.90$ it becomes negative, and does not yield the ρ -meson bound state. (See also Tab. 2.)

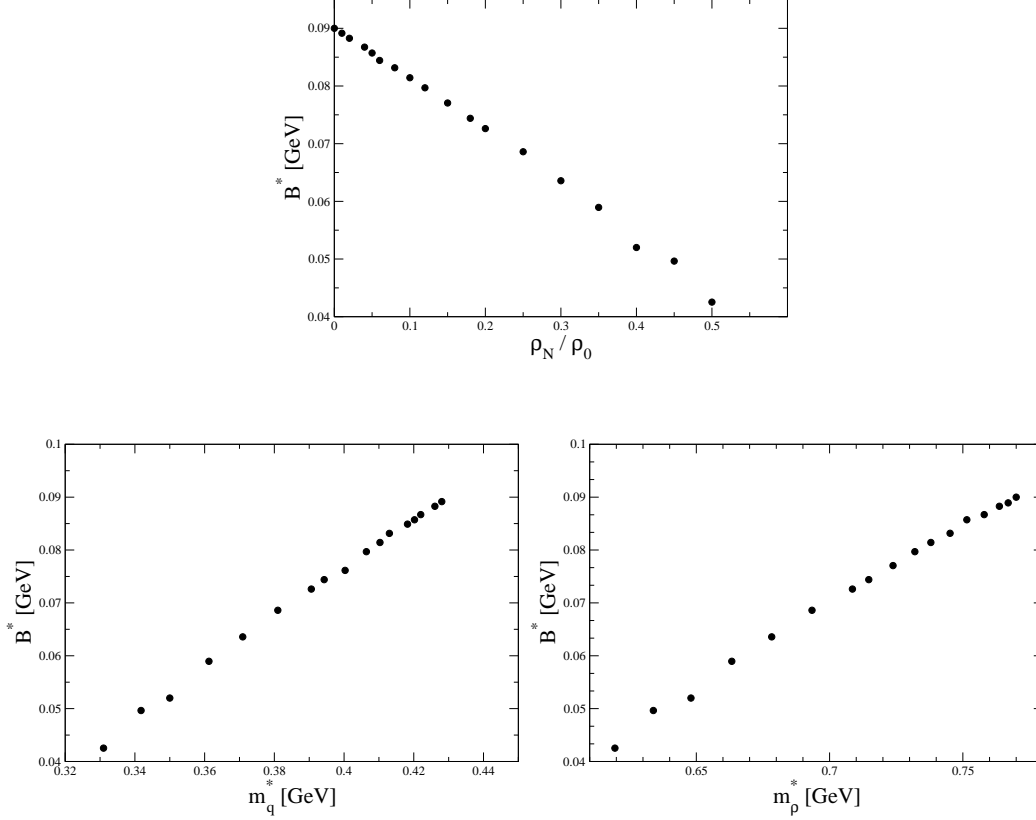


Fig. 2. Binding energy B^* [GeV] of the ρ -meson versus nuclear matter density $[\rho_N/\rho_0]$ (upper panel), versus effective light-quark mass m_q^* [GeV] (lower-left panel), and versus effective ρ -meson mass [GeV] (lower-right panel).

Next, we discuss the ρ -meson electromagnetic decay constant in medium, f_ρ^* . The ρ -meson decay constant gives direct information on the structure of the ρ -meson bound state wave function at the origin. It is associated with the non-perturbative regime of QCD. The ρ -meson decay constant is calculated via Eq. (19) (see also Ref. [18]). However, the experimental data for ρ -meson in vacuum are very scarce [73] compared with those of the other light mesons such as pion [8]. The parameters of the model are fitted to the empirically extracted ρ -meson decay constant from the decay width in vacuum [73,75] (see also Tab. 2). Namely, the light-quark (= light-antiquark) mass of $m_q = 0.430$ GeV, and the regulator mass $m_R = 3.0$ GeV. Using these values, the ρ -meson decay constant in vacuum obtained is $f_\rho = 153.657$ MeV, close to the empirical value of 152 ± 8 MeV [73]. Note that the value of the regulator mass $m_R = 3.0$ GeV in vacuum, will be kept the same in medium to reduce the number of parameters, and since we have no clue for this value in medium. To calculate the in-medium decay constant f_ρ^* , we use the in-medium modified polarization vector $\epsilon_{\lambda=z}^{*\mu}$ (but $\lambda = z$ is unmodified in medium), ρ -meson effective mass m_ρ^* , and effective quark mass m_q^* in evaluating the both sides of Eq. (19).

We show in Fig. 3 (left panel) the density dependence of the ρ -meson decay

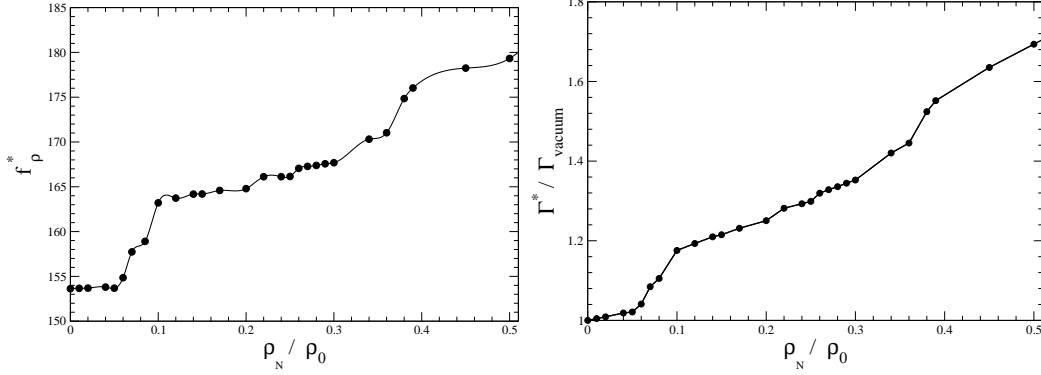


Fig. 3. Density dependence of the ρ -meson decay constant f_ρ^* (left panel), and the density dependence of the decay width ratio, $\Gamma^*(\rho^0 \rightarrow e^+e^-) / \Gamma(\rho^0 \rightarrow e^+e^-)$ (right panel), where $\Gamma(\rho^0 \rightarrow e^+e^-) = 7.04 \pm 0.06$ keV [73] in vacuum.

constant in medium f_ρ^* . The solid line is an interpolated line to be able to see easier the density dependence. At first sight one notices that the density dependence of f_ρ^* is not smooth compared to that of the binding energy B^* in Fig. 2 (upper panel). As we will show later, this feature is also noticeable compared with the density dependence of the ρ -meson electromagnetic form factors and the square charge radius, which have smooth density dependence. However, together with the f_ρ^* values given in Tab. 2, one can conclude that f_ρ^* increases as the nuclear matter density increases. This fact implies that the in-medium ρ^0 -meson decay width to e^+e^- becomes larger, and enhanced further by the reduction of the effective ρ -meson mass m_ρ^* , since the decay width is given by,

$$\Gamma^*(\rho^0 \rightarrow e^+e^-) = \frac{4\pi}{3} \frac{\alpha_e^2}{m_\rho^{*2}} f_\rho^{*2}, \quad (24)$$

where α_e is the electromagnetic fine structure constant. Note that, the increase of f_ρ^* as increasing the nuclear matter density is the opposite behavior from that of the pion decay constant f_π^* [61], which decreases in both the space component and the time component [76] as increasing the nuclear matter density.

In Fig. 3 (right panel) we show the density dependence of the decay width ratio to the vacuum, $\Gamma^*(\rho^0 \rightarrow e^+e^-) / \Gamma(\rho^0 \rightarrow e^+e^-)$, where $\Gamma(\rho^0 \rightarrow e^+e^-) = 7.04 \pm 0.06$ keV [73] in vacuum. As expected, the in-medium decay width for $\rho^0 \rightarrow e^+e^-$ increases as increasing the nuclear matter density. Based on a vector-meson dominance picture, the increase of the decay width in medium $\Gamma^*(\rho^0 \rightarrow e^+e^-)$ relative to that in vacuum, may be interpreted that the ρ -meson fluctuation to the virtual photon γ^* increases in nuclear medium. This behavior of increasing f_ρ^* with the increase of the square charge radius $\langle r_\rho^{*2} \rangle$ which will be shown later in Fig. 5, is consistent with the correlation observed in Ref. [41] in vacuum.

Now we discuss the main results of this article, ρ -meson electromagnetic form

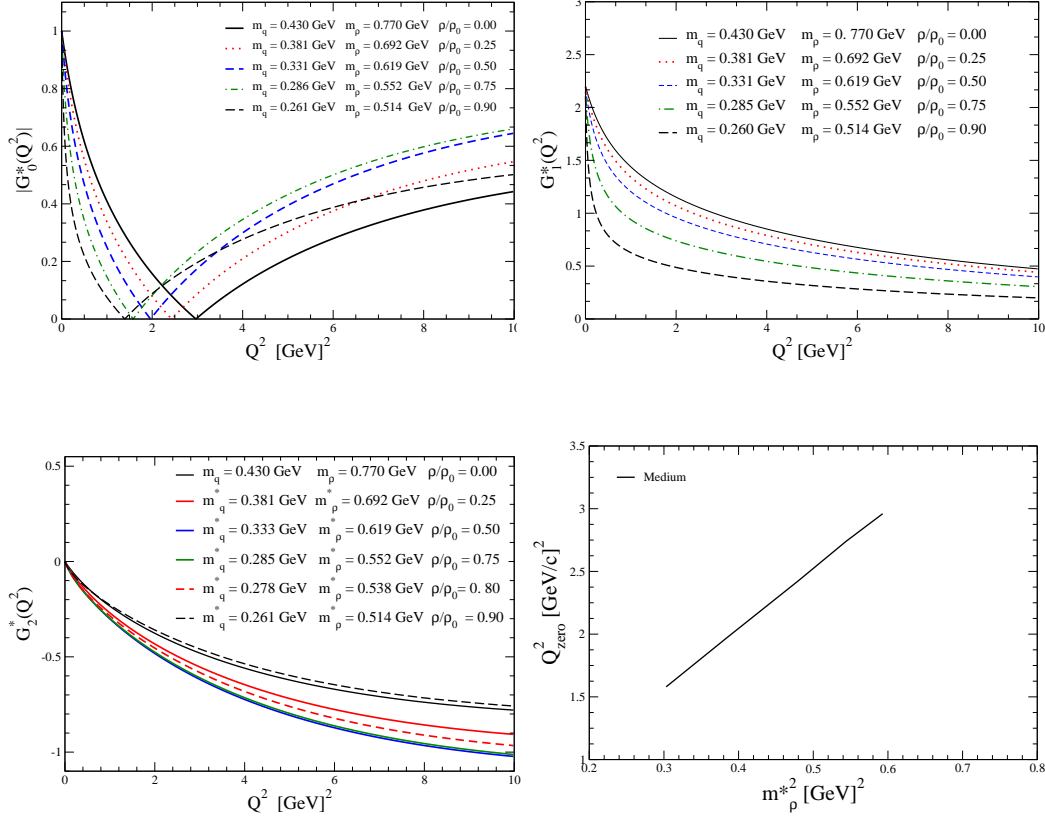


Fig. 4. ρ -meson electromagnetic charge $|G_0|$ (upper left), magnetic G_1 (upper-right panel), and quadrupole G_2 (lower-left panel) form factors for several densities, and the Q_{zero}^2 for $G_0(Q_{\text{zero}}^2) = 0$ versus m_ρ^{*2} (lower-right panel) in symmetric matter.

factors in symmetric nuclear matter. In Fig. 4 we show the ρ -meson charge $|G_0(Q^2)|$ (upper-left panel), magnetic $G_1(Q^2)$ (upper-right panel), quadrupole $G_2(Q^2)$ (lower-left panel) form factors for several nuclear matter densities, and the zero, $Q_{\text{zero}}^2 = -q_{\text{zero}}^2$, to give $G_0(Q_{\text{zero}}^2) = 0$ for the charge form factor, versus the effective ρ -meson mass m_ρ^{*2} (lower-right panel).

The ρ -meson electromagnetic form factors in symmetric nuclear matter G_0^* , G_1^* and G_2^* are strongly modified as increasing the nuclear matter density. The modification of $|G_0^*|$ shows two distinct features: (i) faster decrease near $Q^2 = 0$ relative to that in vacuum, implies the increase of the charge radius in symmetric nuclear matter, and (ii) the position of Q_{zero}^2 decreases as increasing the nuclear matter density almost linearly. The present model has $Q_{\text{zero}}^2 \simeq 3$ GeV² in vacuum [35], where in the literature the values in vacuum are spread in the region, $3 \text{ GeV}^2 < Q_{\text{zero}}^2 < 5 \text{ GeV}^2$ [28,36,37,42,48,74,77]. The fact that G_0 has the zero, is similar to the spin-one deuteron case, a composite system of spin-1/2 particles of proton and neutron [72,78,79]. Other form factors G_1^* and G_2^* also decrease faster than those corresponding form factors in vacuum as increasing the nuclear matter density.

The Q_{zero}^2 versus m_ρ^{*2} shown in the lower-right panel in Fig. 4 is very interesting and may be noticeable. The position of Q_{zero}^2 in terms of m_ρ^{*2} can be expressed by,

$$Q_{\text{zero}}^2 \simeq 5.0 \times m_\rho^{*2} + c, \quad (25)$$

with the constant $c \simeq 0$.

For the ρ -meson magnetic moment in medium $\mu_\rho^* = G_1^*(0)$, the medium modification is the very small quenching (see Tab. 2). In vacuum, $\mu_\rho = 2.20$ in the present model [35,75] (and $\mu_\rho = 2.16$ in Ref. [80]), while $\mu_\rho^* = 2.10$ at $\rho_N/\rho_0 = 0.90$. This is in contrast with the nucleon case, which has been demonstrated to be enhanced as increasing the nuclear matter density [24,81]. This is probably due to the differences in the Lorentz structure between the spin-1 and spin-1/2 particles (see Eqs. (7) and (21)).

The ρ -meson quadrupole moment $Q_{2\rho}$ calculated via Eq. (22), is also sensitive to the effects of the nuclear medium (see Tab. 2). The quadrupole form factor G_2^* shown in Fig. 4 (lower-left panel), changes behavior from quenching to enhancement for the densities larger than $\rho/\rho_0 = 0.75$. The enhancement of the quadrupole moment $Q_{2\rho}^*$ as increasing the nuclear matter density (see Tab. 2), means that the ρ -meson electromagnetic charge distribution deviates more from spherical symmetry in symmetric nuclear matter.

Next, we discuss the ρ -meson electromagnetic square charge radius in symmetric nuclear matter $\langle r_\rho^{*2} \rangle$ calculated with Eq. (23). The results are shown in Fig. 5, versus nuclear matter density (upper panel), versus the effective quark mass m_q^* (lower-left panel), and versus the effective ρ -meson mass m_ρ^* (lower-right panel). The solid line in each panel is a line obtained by fitting to the points calculated, for helping to see easier.

As for the upper panel in Fig. 5 the solid line is obtained by the following expression for the range $0 \leq y \equiv \rho_N/\rho_0 \leq 0.9$,

$$\langle r_\rho^{*2}(y) \rangle = C_0 y^2 + C_1 y + C_2 = 1.24173y^2 - 0.0943938y + 0.286568, \quad (26)$$

where $C_{0,1,2}$ above are all in $[\text{fm}^2]$.

For the lower-left panel in Fig. 5, the fit function is obtained for the region $0.2 \text{ GeV} \leq m_q^* \leq 0.5 \text{ GeV}$ as,

$$\langle r_\rho^{*2}(m_q^*) \rangle = \frac{a_0}{m_q^* - a_1} = \frac{0.049064}{m_q^* - 0.233531}, \quad (27)$$

with a_0 in $[\text{GeV fm}^2]$ and a_1 in $[\text{GeV}]$.

For the lower-right panel in Fig. 5, the fit function for the region $0.50 \text{ GeV} \leq$

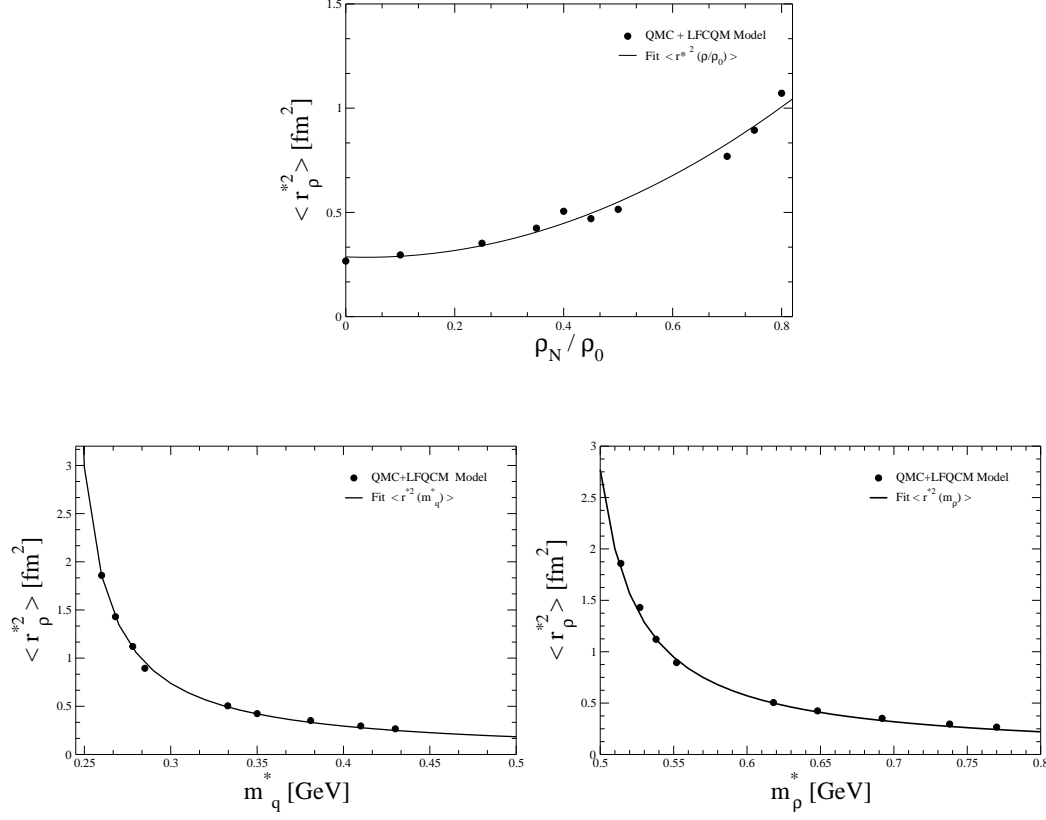


Fig. 5. ρ -meson electromagnetic square charge radius as well as the fitted curves, versus nuclear matter density $[\rho_N/\rho_0]$ (upper panel), versus effective quark mass m_q^* (lower-left panel), and versus effective ρ -meson mass m_ρ^* .

$m_\rho^* \leq 0.80$ GeV obtained is,

$$\langle r_\rho^{*2}(m_\rho^*) \rangle = \frac{b_0}{m_\rho^* - b_1} = \frac{0.0720}{m_\rho^* - 0.474}, \quad (28)$$

with b_0 in $[\text{GeV fm}^2]$ and b_1 in $[\text{GeV}]$.

Three features shown in Fig. 5 for $\langle r_\rho^{*2} \rangle$ can be understood as follows. As the nuclear matter density increases, the charge form factor G_0^* decreases faster near around $Q^2 = 0$ as shown in Fig. 4 upper-left panel, and the derivative with respect to Q^2 becomes negatively larger at $Q^2 = 0$ (see Eq. (23)) to yield larger $\langle r_\rho^{*2} \rangle$. As increasing the nuclear matter density, both m_q^* and m_ρ^* decrease as shown in Fig. 1 lower-left and lower-right panels, respectively. Furthermore, as the nuclear matter density increases, m_q^* , m_ρ^* as well as the binding energy B^* decrease as shown in Fig. 2. The decrease in the binding energy yields a looser bound state, thus resulting in the increase of $\langle r_\rho^{*2} \rangle$.

5 Summary and conclusion

We have studied the ρ -meson electromagnetic properties in symmetric nuclear matter with a light-front constituent quark model using the in-medium inputs calculated by the quark-meson coupling model. Similar approach was already applied in the studies of the pion, kaon, and nucleon properties in symmetric nuclear matter.

First, we predict the increase of the ρ -meson electromagnetic ($\rho^0 \rightarrow e^+e^-$) decay constant, as well as the increase of the electromagnetic decay width as increasing the nuclear matter density. The latter is enhanced further by the decrease of the effective ρ -meson mass in-medium.

The ρ -meson electric, magnetic, and quadrupole form factors are predicted to vary faster in symmetric nuclear matter as increasing the nuclear matter density than those in vacuum, versus the (negative of) four-momentum squared.

Second, we predict that, as increasing the nuclear matter density, the ρ -meson charge radius and modulus of the quadrupole moment increase (enhanced), while the magnetic moment is slightly quenched. The quenching of the magnetic moment is opposite behavior compared with that of the spin-1/2 Dirac particle (known to be enhanced), probably due to the difference in the Lorentz structure. The enhancement of the quadrupole moment in symmetric nuclear matter means that the ρ -meson charge distribution is more deviate from spherical symmetry in symmetric nuclear matter. Furthermore, we predict the value of “zero”, the value of the (negative of) four-momentum transfer squared to cross zero of the ρ -meson charge form factor (positive value), becomes smaller as increasing the nuclear matter density.

Although the present situation does not allow us to have many experimental data in vacuum as well as in nuclear medium, we hope further advances in experiments will provide us with more data on the ρ -meson properties in vacuum and in a nuclear medium (a nucleus).

For a future prospect, we plan to extend the similar approach to study the in-medium properties of K -, D -, K^* - and D^* -mesons.

Acknowledgements

This work was partially supported by the Fundação de Amparo à Pesquisa do Estado de São Paulo (FAPESP), Brazil, No. 2015/16295-5 (JPBCM), and No. 2015/17234-0 (KT), and Conselho Nacional de Desenvolvimento Científico e Tecnológico (CNPq), Brazil, No. 401322/2014-9 (JPBCM), No.

400826/2014-3 (KT), No. 308025/2015-6 (JPBCM), and No. 308088/2015-8 (KT). This work was part of the projects, Instituto Nacional de Ciência e Tecnologia - Nuclear Physics and Applications (INCT-FNA), Brazil, No. 464898/2014-5, and FAPESP Temático, No. 2017/05660-0.

References

- [1] F. J. Ynduráin, *The Theory of Quark and Gluon Interactions*, Springer Verlag (1983).
- [2] P. Z. Skands, Lecture notes *Introduction to QCD*, CERN-PH-TH-2012-196, arXiv:1207.2389.
- [3] Stanley J. Brodsky, Hans-Christian Pauli and Stephen S. Pinsky, Phys. Rept. **301** (1998) 299.
- [4] J. P. Vary *et al.*, Phys. Rev. C **81** (2010) 035205.
- [5] Zbigniew Dziembowski and Lech Mankiewicz, Phys. Rev. Lett. **58** (1987) 2175.
- [6] J. P. B. C. de Melo, H. W. L. Naus and T. Frederico, Phys. Rev. C **59** (1999) 2278.
- [7] D. Melikhov and S. Simula, Phys. Rev. D **65** (2002) 094043.
- [8] J. P. B. C. de Melo, T. Frederico, E. Pace and G. Salme, Nucl. Phys. A **707** (2002) 399.
- [9] J. P. B. C. de Melo, T. Frederico, E. Pace and G. Salmé, Braz. J. Phys. **33** (2003) 301.
- [10] J. P. B. C. de Melo, T. Frederico, G. Salmé and E. Pace, Phys. Lett. B **581** (2004) 75.
- [11] H. Y. Cheng, C. K. Chua and C. W. Hwang, Phys. Rev. D **69** (2004) 074025.
- [12] T. Huang and X. G. Wu, Phys. Rev. D **70** (2004) 093013.
- [13] V. V. Braguta and A. I. Onischenko, Phys. Rev. **70** (2004) 033001.
- [14] L. M. Salcedo, J. P. B. C. de Melo, D. Hajimichef and T. Frederico, Braz. J. Phys. **34** (2004) 297.
- [15] L. M. Salcedo, J. P. B. C. de Melo, D. Hajimichef and T. Frederico, Eur. Phys. J. A **27** (2006) 213.
- [16] V. A. Karmanov, J.-F. Mathiot and A. V. Smirnov, Phys. Rev. D **75** (2007) 045012.
- [17] J. P. B. C. de Melo, T. Frederico, E. Pace and G. Salmé, Nucl. Phys. A **707** (2002) 399.

- [18] J. P. B. C. de Melo, T. Frederico, E. Pace, and G. Salme, Phys. Rev. D **73** (2006) 074013.
- [19] A. F. Krutov, V. E. Troitsky and N. A. Tsirova, Phys. Rev. C **80** (2009) 055210.
- [20] B. L. G. Bakker, H.-M. Choi and C. R. Ji, Phys. Rev. D **63** (2001) 074014.
- [21] L. S. Kissilinger, H.-M. Choi and C. R. Ji, Phys. Rev. D **63** (2001) 113005.
- [22] Elmar P. Biernat, Franz Gross, M. T. Peña and Alfred Stadler, Phys. Rev. **D89** (2014) 016006.
- [23] G. H. S. Yabusaki, Ishtiaq Ahmed, M. A. Paracha, J. P. B. C. de
- [24] W. R. B. de Arujo, J. P. B. C. de Melo and K. Tsushima, Nucl. Phys. A **970** (2018) 325.
- [25] T. Horn and Craig D Roberts, J. Phys. G **43** (2016) 073001, and references therein.
- [26] Lekha Adhikari, Yang Li, Xingbo Zhao, Pieter Maris, James P. Vary and Alaa Abd El-Hady, Phys. Rev. Rev. **C93** (2016) 055202.
- [27] A. Bacchetta, S. Cotogno and B. Pasquini, Phys. Lett. B **771** (2017) 546.
- [28] F. Cardarelli, I.L.Grach, I.M. Narodetskii, E. Pace, G. Salmé and S. Simula, Phys. Lett. **B349** (1995) 393.
- [29] J. P. B. C. de Melo and T. Frederico, Phys. Lett. B **708** (2012) 87.
- [30] J. P. B. C. de Melo, T. Frederico, H. W. L. Naus and P. U. Sauer, Nucl. Phys. A **660** (1999) 219.
- [31] F. M. Lev, E. Pace and G. Salmé, Phys. Rev. Lett. **83** (1999) 5250.
- [32] F. M. Lev, E. Pace and G. Salmé, Phys. Rev. **C62** (2000) 064004.
- [33] W. Jaus, Phys. Rev. D **67** (2003) 094010.
- [34] T. M. Aliev and M. Savci, Phys. Rev. D **70** (2004) 094007.
T. M. Aliev, A. Özpınec and M. Savci, Phys. Lett. B **678** (2009) 470.
- [35] J. P. B. C. de Melo and T. Frederico, Phys. Rev. **C55** (1997) 2043.
- [36] Ho-Meoyng Choi and Chueng-Ryong Ji, Phys. Rev. **D 70** (2004) 053015.
- [37] M. S. Bhagwat and P. Maris, Phys. Rev. **C 77** (2008) 025203.
- [38] Guidiño, D. García, Sánchez, G. T., Int. J. Mod. Phys. A **30** (2015) no. 18n19, 1550114.
- [39] V. Simonis, Eur. Phys. J. A **52** (2016) no. 4, 90.
- [40] M. E. Carrillo-Serrano, W. Bentz, I. C. Clot and A. W. Thomas, Phys. Rev. C **92** (2015) no. 1, 015212.

- [41] A. F. Krutov, R. G. Polezhaev and V. E. Troitsky, Phys. Rev. D **93** (2016) no. 3, 036007.
- [42] H. L. L. Roberts, A. Bashir, L. X. Gutierrez-Guerrero, C. D. Roberts and D. J. Wilson, Phys. Rev. C **83** (2011) 065206.
- [43] Elmar P. Biernat and Wolfgang Schweiger, Phys. Rev. C **89** (2014) 055205.
- [44] Ho-Meoyng Choi and Chueng-Ryong Ji, Phys. Rev. **D 80** (2014) 033011.
- [45] B. D. Sun and Y. B. Dong, Phys. Rev. D **96** (2017) no. 3, 036019.
- [46] G. M. Huber, G. J. Lolos and Z. Papandreou, Phys. Rev. Lett. **80** (1998) 5285.
- [47] G. M. Huber *et al.* [TAGX Collaboration], Phys. Rev. C **68** (2003) 065202.
- [48] C. Adamuscin, G. I. Gakh and E. Tomasi-Gustafsson, Phys. Rev. C **75** (2007) 065202;
A. Dbeyssi, E. Tomasi-Gustafsson, G. I. Gakh and C. Adamuscin, Phys. Rev. C **85** (2012) 048201.
- [49] J. P. B. C. de Melo, C. R. Ji and T. Frederico, Phys. Lett. B **763** (2016) 87.
- [50] B. Aubert *et al.* [BaBar Collaboration], Phys. Rev. D **78** (2008) 071103.
- [51] W. Jaus, Phys. Rev. **D41**, 3394 (1990); Phys. Rev. **D44** (1991) 2851;
W. Jaus and D. Wyler, Phys. Rev. **D41**, (1990) 3405.
- [52] Wolfgang Jaus, Phys. Rev. **D44** (1991) 2851.
- [53] Ho-Meoyng Choi and Chueng-Ryong Ji, Phys. Rev. D91 (2015) 014018.
- [54] H.-M. Choi, C.-R. Ji, Z. Li, H.-Y. Ryu, Phys. Rev. C **92** (2015) 055203.
- [55] C. Fanelli, E. Pace, G. Romanelli, G. Salmè, M. Salmistraro, Eur. Phys. J. C **76** (2016) 253.
- [56] J. P. B. C. de Melo, T. Frederico, Few Body Syst. **52** (2012) 403.
- [57] J. P. B. C. de Melo, Anacé N. da Silva, Clayton S. Mello and T. Frederico, EPJ Web Conf. 73 (2014) 03017.
- [58] J. P. B. C. de Melo and K. Tsushima, Few Body Syst. **58** (2017) no. 2, 82.
- [59] R. S. Hayano and T. Hatsuda, Rev. Mod. Phys. **82** (2010) 2949.
- [60] W. K. Brooks, S. Strauch and K. Tsushima, J. Phys. Conf. Ser. **299** (2011) 012011.
- [61] J. P. B. C. de Melo, K. Tsushima, B. El-Bennich, E. Rojas and T. Frederico, Phys. Rev. C **90** (2014) no.3, 035201.
- [62] J. P. B. C. de Melo and T. Frederico, Braz. J. Phys. **34** (2004) 881.
- [63] L. Grach and L. A. Kondratyuk, Sov. J. Nucl. Phys. 39, 198 (1984);
L. L. Frankfurt, I. L. Grach, L. A. Kondratyuk, and M. Strikman, Phys. Rev. Lett. 62 (1989) 387.

- [64] J. P. B. C. de Melo, K. Tsushima, and T. Frederico, AIP Conference Proceedings **1735** (2016) 080006.
- [65] J. P. B. C. de Melo, K. Tsushima and I. Ahmed, Phys. Lett. **B766** (2017) 125.
- [66] G. H. S. Yabusaki, J. P. B. C. de Melo, W. de Paula, K. Tsushima and T. Frederico, [arXiv:1712.07176 [hep-ph]].
- [67] P. A. M. Guichon, Phys. Lett. B **200** (1988) 235.
- [68] T. Frederico, B. V. Carlson, R. A. Rego and M. S. Hussein, J. Phys. G **15** (1989) 297.
- [69] P. A. M. Guichon, K. Saito, E. N. Rodionov and A. W. Thomas, Nucl. Phys. A **601** (1996) 349;
K. Saito, K. Tsushima and A. W. Thomas, Nucl. Phys. A **609** (1996) 339; Phys. Rev. C **55** (1997) 2637;
K. Tsushima, K. Saito, J. Haidenbauer and A. W. Thomas, Nucl. Phys. A **630**, 691 (1998);
P. A. M. Guichon, A. W. Thomas and K. Tsushima, Nucl. Phys. A **814** (2008) 66.
- [70] K. Saito, K. Tsushima and A. W. Thomas, Prog. Part. Nucl. Phys. **58** (2007) 1.
- [71] G. Krein, A. W. Thomas and K. Tsushima, arXiv:1706.02688 [hep-ph] to appear in Prog. Part. Nucl. Phys. (2018).
- [72] R. A. Gilman and F. Gross, J. Phys. G **28** (2002) R37;
F. Gross, Phys. Rev. **134** (1964) no.2B, B405;
F. Gross, Phys. Rev. **136** (1964) B140.
- [73] K. A. Olive, Particle Data Group; The Review of Particle Physics. Chin. Phys. C38 (2014) 090001.
- [74] B. L. G. Bakker, H. M. Choi and C. R. Ji, Phys. Rev. D **65** (2002) 116001.
- [75] Clayton S. Mello, Anacé N. da Silva, J. P. B. C. de Melo, T. Frederico, Few-Body Syst. **56** (2015) no.6-9, 509.
- [76] M. Kirchbach and A. Wirzba, Nucl. Phys. A **616** (1997) 648.
- [77] J. P. B. C. de Melo, in preparation.
- [78] A. Buchmann, Y. Yamauchi and A. Faessler, Nucl. Phys. A **496** (1989) 621.
- [79] C. E. Carlson, Nucl. Phys. A **508** (1990) 481.
- [80] A. F. Krutov, R. G. Polezhaev and V. E. Troitsky, arXiv:1801.01458 [hep-ph].
- [81] D. H. Lu, K. Tsushima, A. W. Thomas, A. G. Williams and K. Saito, Phys. Rev. C **60** (1999) 068201.